

Cite this: *Chem. Sci.*, 2025, **16**, 21416

All publication charges for this article have been paid for by the Royal Society of Chemistry

Received 17th July 2025
Accepted 27th September 2025

DOI: 10.1039/d5sc05329c
rsc.li/chemical-science

Introduction

Anilines are ubiquitous structural motifs in bioactive molecules.^{1,2} The physicochemical properties and function of anilines are dictated by the nature and the positioning of their substituents.^{3–5} Changes in substitution patterns profoundly impact interactions with biological targets by modulating H-bonding, π -stacking, and other non-covalent interactions.^{6,7} Thus, positional isomers of anilines often display distinct biological profiles, underscoring the importance of accessing such variants during structure–activity relationship campaigns. Despite this relevance, accessing all possible isomeric aromatic compounds can still be challenging and, in most cases, each derivative requires a specifically designed and optimized *de novo* synthesis. This is due to the nature of traditional aromatic amination that follows a linear sequence of synthetic steps where functionality precursors (e.g. nitro group for reduction)^{8–10} or reactivity handles (e.g. halides for Buchwald–Hartwig cross-coupling) are installed *via* electrophilic aromatic substitution.^{11–14} Although more modern radical-based methods offer a more direct approach, they generally afford only a single isomer (*para*) and do not overcome the limitations in regioisomeric diversification (*ortho* – *meta*).^{15–20} A highly desirable yet underexplored strategy involves the direct translocation of functional groups from one aromatic position to another. This would bypass traditional synthetic limitations and facilitate access to

^aInstitute of Organic Chemistry, RWTH Aachen University, Landoltweg 1, Aachen, 52074, Germany. E-mail: daniele.leonori@rwth-aachen.de

^bDepartment of Chemistry, Faculty of Science, Gazi University, Teknikokullar, Ankara, 06500, Turkey

^cOtto Diels – Institute of Organic Chemistry, Christian Albrecht Universität zu Kiel, Otto-Hahn-Platz 4, 24188 Kiel, Germany. E-mail: aruffoni@oc.uni-kiel.de

† These authors contributed equally to this work.

A photochemical strategy for aromatic nitrogen *ortho*-isomerization

Giovanni Lenardon, †^a Xheila Yzeiri, †^a Gael Le Berre,^a Dilara Berna Yıldız,^{ab} Daniele Leonori ^a and Alessandro Ruffoni ^{bc}

Anilines are essential functional groups in bioactive molecules. Their aromatic substitution pattern governs key physicochemical properties and thus biological activity. Accessing anilines with identical substituents but at alternative aromatic positions is highly desirable, but remains synthetically challenging. Herein, we report a synthetic strategy enabling the *ortho*-isomerization of aromatic nitrogen substituents. This approach leverages the visible light-mediated decomposition of aryl azides in the presence of a tailored thiophenol reagent to generate *ortho*-aminothiophenols. This transformation proceeds *via* nitrene generation and insertion, relocating the nitrogen group to its *ortho* position while installing the sulfur moiety at the *ipso* site. Subsequent oxidative cyclization yields a cyclic sulfonium intermediate, which can be cleaved or exploited as linchpins for divergent functionalization.

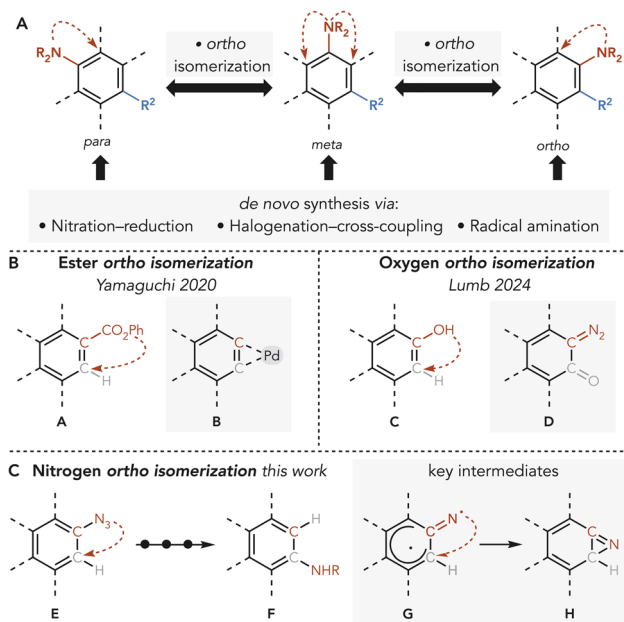
high-value isomers. Unfortunately, methods that achieve such rearrangements are rare.^{21–23} The classical “halogen dance” strategy is limited to heteroaromatics^{24,25} and fails with benzenoids.^{26–29} Very recently, work by Yamaguchi and Lumb has explored new approaches to achieving aromatic *ortho*-isomerization. Yamaguchi developed a Pd-catalyzed process for the reconfiguration of ester groups **A** leveraging the thermodynamic equilibrium of η^2 -aryne–palladium complexes **B** during carbonylation and elimination steps (Scheme 1B).^{30,31} Lumb enabled the *para* to *meta* migration of OH groups in phenols **C** employing a designed sulfonyl hydrazide reagent to selectively generate diazonium intermediates **D** (Scheme 1B).³² These methods are restricted to single positional shifts without enabling further isomerization. Here, we report a synthetic protocol for nitrogen *ortho*-isomerization on benzene rings (Scheme 1C). Our approach uses aryl azides and a tailored thiophenol reagent under visible-light photolysis to generate singlet nitrenes, which undergo regioselective insertion to yield *ortho*-aminothiophenols. These intermediates are converted to sulfonium salts, which serve as both removable handles and diversification platforms. This protocol enables the isomerization of the nitrogen atom from the *para* to the *meta* position, and from the *meta* to the *ortho* or *para* positions, potentially allowing controlled access to all possible isomers. The strategy is compatible with polysubstituted derivatives and has been applied to the isomerization of bioactive molecules.

Results and discussion

Design plan

In our earlier studies we demonstrated the synthesis of *ortho*-aminothiophenols,³³ upon irradiating aryl azides **I** and sodium





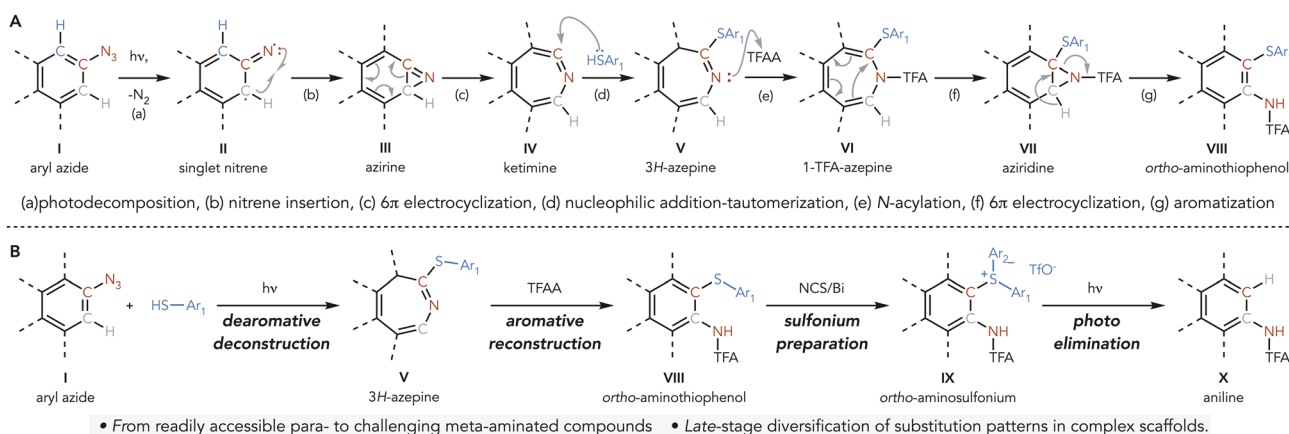
Scheme 1 (A) Group translocation-ortho isomerization logic. (B) Group translocation-ortho isomerization precedent. (C) This work.

thiolates with purple LEDs ($\lambda = 390$ nm) (Scheme 2A).^{33–37} This process generates singlet aryl nitrenes **II**,^{38–43} which undergo N–insertion to form azirines **III**.⁴⁴ These intermediates partake in a 6π-electrocyclization event, leading to highly electrophilic ketimines **IV**. These intermediates can be trapped *in situ* with thiol nucleophiles and the resulting 1*H*-azepines^{45–47} readily isomerize to the thermodynamically stable 3*H*-azepines **V**.^{48–53} When treated with electrophiles like TFAA, **V** were converted into **VII** *via* the generation of antiaromatic **VI**, followed by 6π-electrocyclization^{33,37,54,55} and aromatization. A key mechanistic aspect of this strategy is that the nitrogen undergoes *ortho*-isomerization, with the thiol being selectively trapped at the original *ipso* position of the starting aryl azide **I**. Although this methodology effectively relocates the nitrogen atom, it fails to deliver rearranged anilines due to sulfur incorporation in the

final product. We envisioned that conversion of these amino-thiophenols into sulfonium species followed by visible-light-mediated cleavage could provide a route to the rearranged anilines (Scheme 2B).

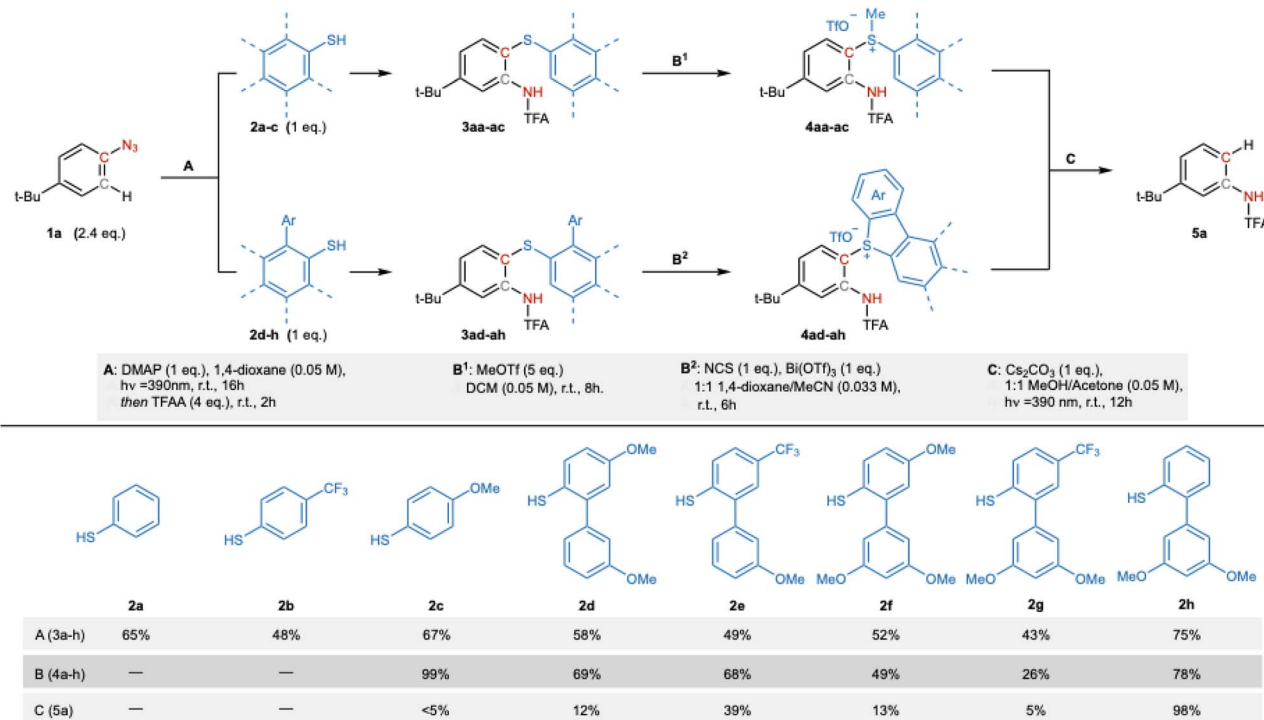
Reaction development

The success of this concept hinged on identifying a thiophenol capable of both trapping the ketimine intermediate and supporting subsequent sulfonium formation for the final cleavage step. Building on our previous work, we began by evaluating thiols **2a** and **2b**, which successfully enabled the formation of *ortho*-aminothiophenols.³³ However, these intermediates failed to generate the corresponding sulfonium salts, likely due to the insufficient nucleophilicity of the sulfur moiety. In contrast, the more electron-rich thiol **2c** afforded the desired sulfonium in high yield, but attempts at photoinduced cleavage were unsuccessful. These results clearly underscored the need for a single thiophenol reagent that could efficiently support all three steps of the sequence. To address this, we explored *ortho*-aryl-substituted thiophenols, which were expected to form cyclic triaryl sulfoniums. These species were of particular interest due to their known propensity for undergoing photofragmentation with release of dibenzothiophene.^{56–59} Accordingly, we evaluated a series of biaryl thiophenols (**2d–2h**, Scheme 3). However, under standard conditions, these derivatives failed to participate in the nitrene-based insertion reaction. We found that their conversion to the corresponding sodium salts, required to activate the thiol for ketimine trapping, resulted in significant decomposition, presumably due to their high electron density and susceptibility to oxidative degradation. Since these thiophenols showed no reactivity in the absence of a base, we re-optimized the nitrene-insertion step. Rather than using a strong base, which can readily generate easily oxidized thiolates, we investigated the use of a milder base that could potentially also act as a nucleophilic activator. This base may trap the ketimine intermediate, thereby enabling its subsequent displacement by the sulfide. This approach proved effective, and DMAP was identified as the



Scheme 2 (A) Proposed mechanistic blueprint for the photochemical conversion of aryl azides into *ortho*-aminothiophenols. (B) Synthetic strategy design for nitrogen *ortho* isomerization.





Scheme 3 Optimized reaction conditions & thiol reagent design.

optimal additive to facilitate capture of intermediate **IV** by thiophenols **2d–2h**.

Among these, thiophenol **2h** gave the highest conversion, whereas derivatives bearing para electron-donating (OMe, compounds **2d** and **2f**) or electron-withdrawing (CF₃, compounds **2e** and **2g**) substituents displayed reduced reactivity. With this improved protocol, we next examined sulfonylum formation: upon treatment with MeOTf in DCM (conditions **B²**) only substrate **3ac** was successfully converted to the desired product, which then unfortunately failed to undergo the subsequent step. On the other hand, with NCS as the electrophile and Bi(OTf)₃ as the Lewis acid (conditions **B¹**) we were able to obtain all the corresponding triaryl sulfonium salts, with^{60,61} the derivative derived from thiophenol **2h** affording once again the highest yield. The final photocleavage step was evaluated using purple LEDs ($\lambda = 390\text{ nm}$) in a MeOH-acetone mixture with Cs₂CO₃ as base. Notably, the efficiency of this transformation was highly sensitive to the substitution pattern on the sulfonylum ring. While several sulfonylum derivatives (**2c**, **2d**, **2f** and **2g**) gave poor conversions, the compound derived from thiophenol **2h** underwent clean photofragmentation to deliver the desired translocated aniline in quantitative yield. Although the origins of this enhanced reactivity remain unclear, thiophenol **2h** consistently outperformed all other candidates across each of the three steps and was therefore selected as the optimal reagent for further scope exploration.

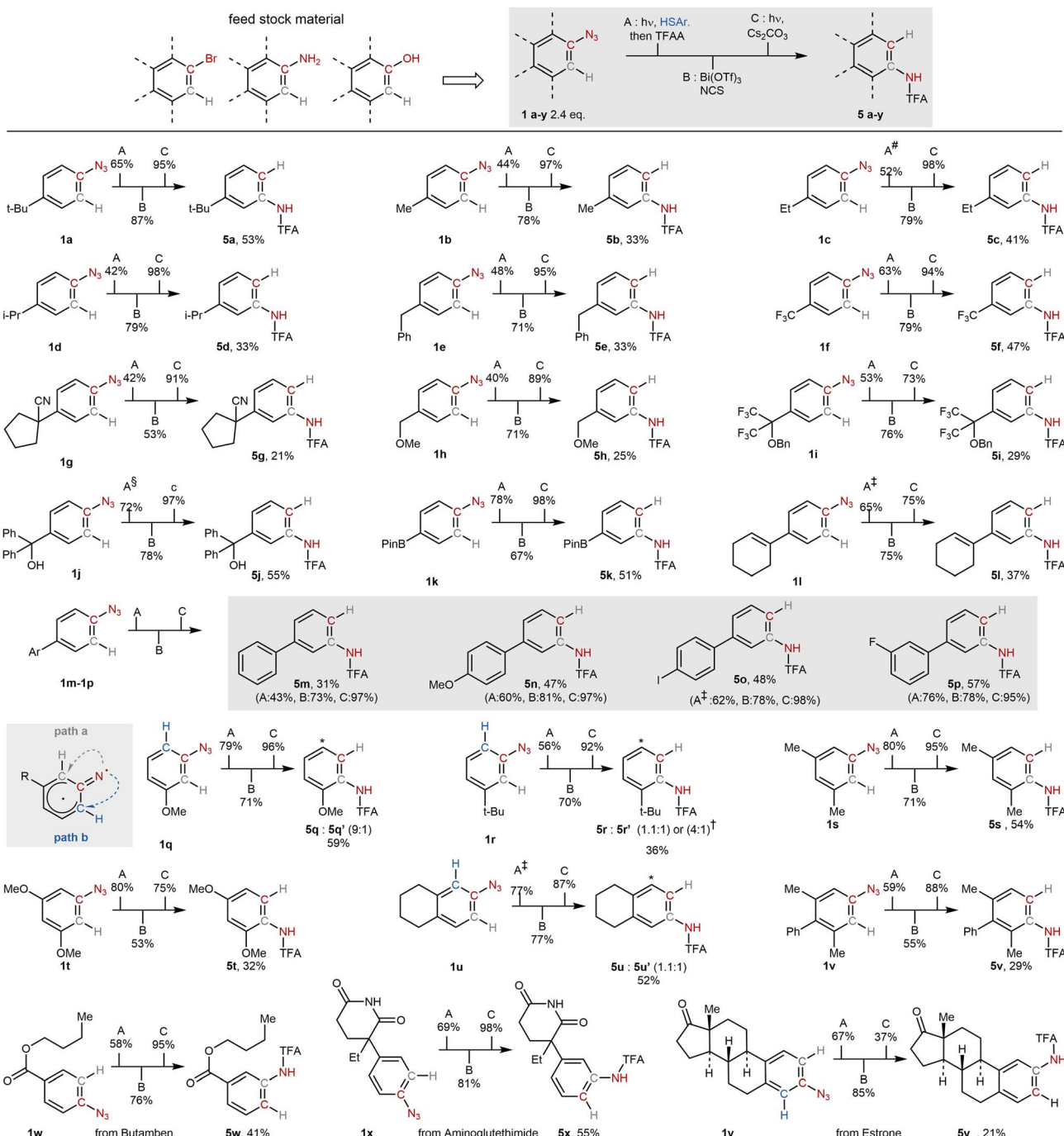
Scope of the nitrogen ring walk

With the optimized reaction conditions in hand, we explored the substrate scope using *para*-substituted aryl azides (**1a–1y**).

These azides, which are readily accessible from the corresponding *para*-substituted anilines as well as other feedstock materials (see SI material for details), serve as valuable precursors to *meta*-functionalized anilines, which are often synthetically challenging to access and, in fact, represent only a small fraction (7%) of commercially available compounds (see SI material for details).

As shown in Scheme 4A, a series of alkyl substituents were well tolerated, delivering products **5b–5e** in overall good yields across the three-step sequence. Importantly, these substituents could incorporate a diverse range of functional groups, including HAT-activated benzyl (**1e**), α -methoxy (**1h**), nitrile-substituted quaternary carbons (**1g**), and trifluoromethyl groups (**1f**, **1i**). These products (**5g–5i**) were obtained in slightly reduced yields. Free alcohols, as in aryl azide **1j**, afford **5j** in 55% yield, with no observed self-condensation during the initial step, highlighting the protocol's chemoselectivity for thiol nucleophiles. Notably, the strongly electron-withdrawing *para*-CF₃ group (**1f**) was compatible, affording **5f** in 47% overall yield. A boronic ester [B(pin)] substituent was also tolerated, furnishing product **5k**, which is amenable to downstream cross-coupling functionalization. We next examined substrates bearing alkene (**1l**) and aromatic (**1m–1p**) groups. These furnished the corresponding anilines (**5l–5p**) in moderate to good yields and demonstrated compatibility with *para*-substituents such as methoxy, iodine, and fluorine. This is particularly noteworthy given that *para*-substituted aromatics are known to suppress nitrene insertion due to electronic deactivation.⁶² With *meta*-substituted azides, mixtures of *ortho*- and *para*-products were observed, consistent with the possibility of nitrene



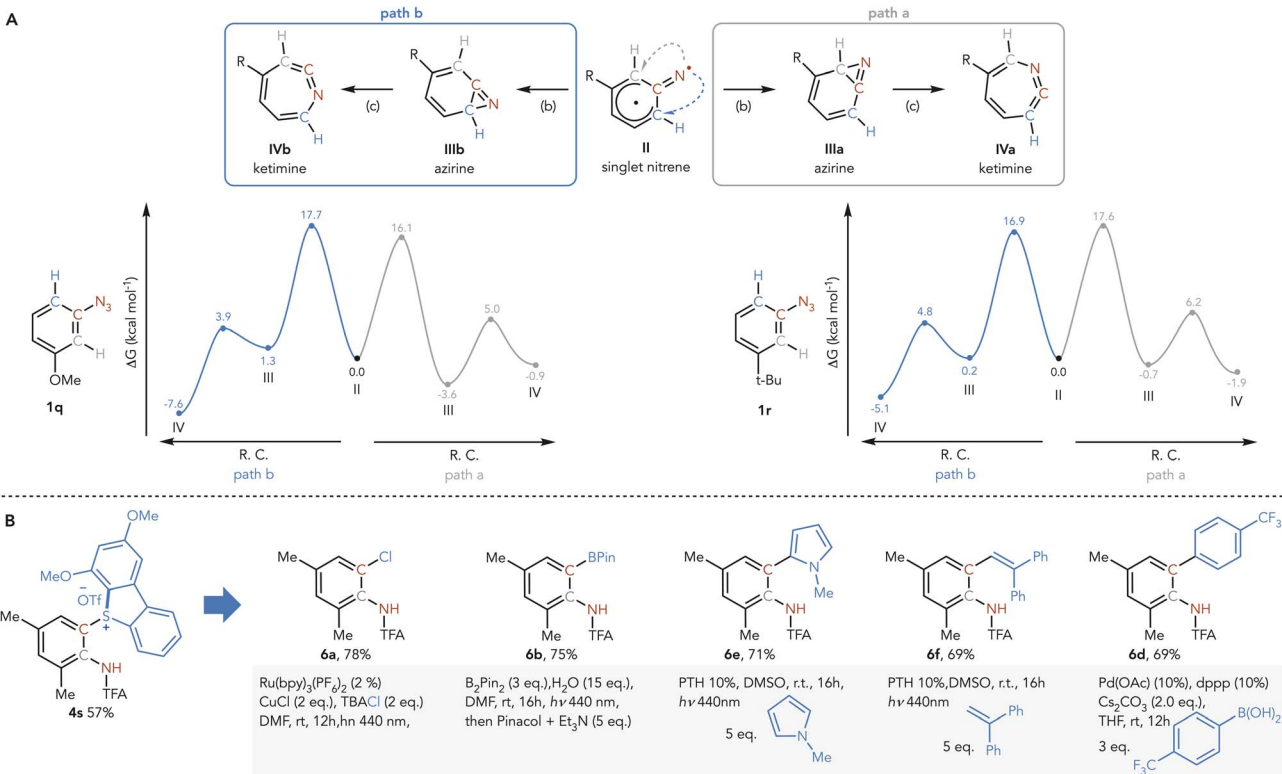


Scheme 4 Substrate scope of the nitrogen *ortho* isomerization. Solvent: # hexane, § diethyl ether, ‡ trifluorotoluene, † step A: trifluorotoluene 60 °C. Conditions: A: DMAP (1 eq.), 1,4-dioxane (0.05 M), $h\nu$ = 390 nm, r.t., 16 h, then TFAA (4 eq.), r.t., 2 h. B: NCS (1 eq.), $Bi(OTf)_3$ (1 eq.), 1 : 1,4-dioxane/MeCN (0.033 M), r.t., 6 h. C: Cs_2CO_3 (1 eq.), 1 : 1 MeOH/Acetone (0.05 M), $h\nu$ = 390 nm, r.t., 12 h. Yield: A = yield calculated based on the amount of thiol used, A and B = NMR yield, C = isolated yield.

cyclization at either *ortho* position (Scheme 3).⁶³⁻⁶⁶ Nonetheless, the OMe-containing azide **1q** showed high regioselectivity for the *ortho*-isomer **5q**. In contrast, the *tert*-butyl derivative **1r** gave a near 1 : 1 mixture of *ortho* and *meta* products. Remarkably, shifting the solvent to trifluorotoluene and conducting the reaction at 60 °C significantly enhanced regioselectivity, yielding the *ortho*-isomer **5r** in a 4 : 1 ratio. (See the SI material for details of the optimization and comprehensive studies on

other substrates) This observation highlights the decisive influence of solvent polarity and temperature on the reaction coordinate, allowing for fine-tuning of positional selectivity (Scheme 5A).

We further extended the scope to polysubstituted azides. Symmetrical di-*meta*-substituted derivatives **1s** and **1t** yielded *ortho*-*para* anilines **5s** and **5t** in 54% and 32% yields, respectively, showcasing the method's tolerance toward electronically



Scheme 5 (A) Mechanistic analysis of regioselectivity. The numbers are the relative Gibbs free energies at UM06-2X/def2-QZVPP//def2-TZVP level of theory (kcal mol⁻¹). (B) Synthesis of *ortho*-anilines via sulfonium diversification.

rich systems. The bicyclic 6-azido-tetrahydronaphthalene **1u** provided both regioisomers in comparable yields (36% and 52%). Trisubstituted azide **1v** enabled the synthesis of the tetrasubstituted aniline **5v** in 29% yield, an otherwise synthetically demanding structure that lies beyond the reach of conventional S_EAr or cross-coupling strategies.⁵ To further demonstrate the synthetic utility of our strategy, we applied it to azide derivatives of bioactive compounds. The local anesthetic butamben was converted into *meta*-butamben **5w** in 27% yield. Similarly, the anticancer agent aminoglutethimide underwent clean *para*-to-*meta* isomerization to afford **5x** in 55% yield. Estrone-derived azides yielded a 1:1 mixture of isomerized aminothiophenol intermediates. However, despite efficient sulfonium formation, photochemical cleavage conditions led exclusively to product **5y** in 21% yield, with the other regioisomer undergoing complete decomposition.⁶⁷ It is worth noting that TFA protection is generally removed quantitatively after treatment with aqueous KOH wash, delivering the free anilines. This results in an overall isomerization from *para*-aniline (azide precursors) to *meta*-anilines.

Mechanistic analysis of regioselectivity

To gain deeper insight into the origins of regioselectivity in *meta*-substituted aryl azides such as **1q** and **1r**, we carried out DFT calculations on the two pathways (path a and path b) that proceed from the singlet nitrene (II) to the ketimine (IV) via the azirine (III), as the regioselectivity of the reaction is determined

by the nitrene insertion (Scheme 5A). For **1q**, the nitrene-to-azirine conversion (step b) is clearly favored along path a: the computed barrier is lower (16.1 vs. 17.1 kcal mol⁻¹), and the resulting azirine intermediate is more stabilized (-3.6 vs. 1.3 kcal mol⁻¹). This dual kinetic and thermodynamic advantage renders path a the dominant trajectory, providing a straightforward rationale for the regioselectivity observed experimentally. In the case of **1r**, however, the situation is more nuanced. The two transition states are separated by less than 1 kcal mol⁻¹, and the corresponding azirine intermediates differ only slightly in stability (path a favored by 0.9 kcal mol⁻¹). The combination of a slightly lower barrier for the path b azirine and the greater stability of the path a azirine establishes a kinetic-thermodynamic dichotomy: the path b azirine can be classified as the kinetic product, while the path a analogue represents the thermodynamic minimum. This balance provides a natural rationale for the temperature-dependent outcome: under ambient conditions both azirines may form in comparable amounts, whereas the elevated temperature equilibration shifts the distribution toward the thermodynamically preferred path a.

Synthesis of *ortho*-aniline

Aryl sulfoniums are powerful synthetic handles for diverse functionalization *via* cross-coupling reactions and redox chemistry.^{68–74} The sulfonium group can be introduced onto the aromatic ring either by exploiting existing



prefunctionalization^{68,73} or directly *via* C–H functionalization, typically with para-selectivity.^{69,72,74} Our protocol allows the selective installation of sulfonyl groups *ortho* to aniline functionalities with complete regiocontrol. We envisaged that this intermediate could act as a strategic platform to enable divergent *ortho*-functionalization pathways, expanding the reactivity beyond nitrogen isomerization. This concept was validated as shown in (Scheme 5B). Photoredox-induced fragmentation in the presence of a chlorinating agent provided *ortho*-chloroaniline **6a** in 69% yield.²² Similarly, blue light irradiation ($\lambda = 440$ nm) in the presence of $B_2(\text{pin})_2$ afforded *ortho*-borylated product **6b** in 75% yield, enabling further downstream diversification through standard cross-coupling protocols.⁶⁹ Furthermore, phenylphenothiazine (PTH)-mediated reduction of sulfonyl **4t** generated an aryl radical intermediate that was effectively intercepted by methylpyrrole and styrene to afford C–C coupled products **6c** and **6d** in 71% and 69% yields, respectively. Finally, the versatility of these sulfonyl intermediates was showcased through a Suzuki–Miyaura cross-coupling reaction, delivering *ortho*-arylated aniline **6e** in 69% yield.

Conclusions

We have developed a synthetic strategy for *ortho*-isomerization of aromatic nitrogen. This method enables the transformation of easily accessible *para*-substituted anilines into more challenging *meta*-functionalized derivatives. This protocol tolerates many functionalities often encountered in organic synthesis and has proven efficient for late-stage reconfiguration of bioactive molecules. We hope this might find application as a tool for chemical space exploration without the requirement for *de novo* synthesis. Furthermore, the sulfonyl intermediates generated as part of the strategy can serve as a powerful linchpin for diverse transformations, including photoredox catalysis and cross-coupling. This can be used to overcome current limitations in aniline functionalization chemistry and expand the scope of accessible derivatives.

Author contributions

AR and DL conceptualized, designed, and supervised the project. GL, XY and GLB performed all the synthetic experiments. DBY performed the computational experiments. All authors analysed the results and wrote the manuscript.

Conflicts of interest

There are no conflicts to declare.

Data availability

The data that support the findings of this study are available in the supplementary information (SI) of this article. Supplementary information is available. See DOI: <https://doi.org/10.1039/d5sc05329c>.

Acknowledgements

D. L. thanks the ERC for a grant (101086901). G. L. and X. Y. contributed equally to this work. The manuscript was written through contributions of all authors. All authors have given approval to the final version of the manuscript. DBY acknowledges the financial support of the Study Abroad Postgraduate Education Scholarship (YLSY) awarded by the Republic of Türkiye Ministry of National Education. The numerical calculations reported in this paper were fully performed at TUBITAK ULAKBIM, High Performance and Grid Computing Center (TRUBA resources). Also, I notices that the zip file containing the cartesian coordinates and thermodynamic data doesn't appear in the Supporting Information section.

Notes and references

- 1 S. D. Roughley and A. M. Jordan, *J. Med. Chem.*, 2011, **54**, 3451–3479.
- 2 E. Vitaku, D. T. Smith and J. T. Njardarson, *J. Med. Chem.*, 2014, **57**, 10257–10274.
- 3 K. C. Gross and P. G. Seybold, *Int. J. Quantum Chem.*, 2000, **80**, 1107–1115.
- 4 C. Hansch, A. Leo and R. W. Taft, *Chem. Rev.*, 1991, **91**, 165–195.
- 5 A. Nilova, L.-C. Campeau, E. C. Sherer and D. R. Stuart, *J. Med. Chem.*, 2020, **63**, 13389–13396.
- 6 A. Ricci, *Amino group chemistry: from synthesis to the life sciences*, John Wiley & Sons, 2008.
- 7 S. Burley and G. A. Petsko, *Science*, 1985, **229**, 23–28.
- 8 S. Liu, Z. Gan, M. Jiang, Q. Liao, Y. Lu, H. Wang, Z. Xue, Z. Chen, Y. Zhang and X. Yang, *JACS Au*, 2024, **4**, 4899–4909.
- 9 S. Patra, I. Mosiagin, R. Giri and D. Katayev, *Synthesis*, 2022, **54**, 3432–3472.
- 10 G. A. Olah, S. C. Narang, J. A. Olah and K. Lammertsma, *Proc. Natl. Acad. Sci. U. S. A.*, 1982, **79**, 4487–4494.
- 11 I. P. Beletskaya and A. V. Cheprakov, *Coord. Chem. Rev.*, 2004, **248**, 2337–2364.
- 12 J. F. Hartwig, *Nature*, 2008, **455**, 314–322.
- 13 P. Ruiz-Castillo and S. L. Buchwald, *Chem. Rev.*, 2016, **116**, 12564–12649.
- 14 M. J. West, J. W. Fyfe, J. C. Vantourout and A. J. Watson, *Chem. Rev.*, 2019, **119**, 12491–12523.
- 15 L. Legnani, G. Prina Cerai and B. Morandi, *ACS Catal.*, 2016, **6**, 8162–8165.
- 16 G. B. Boursalian, W. S. Ham, A. R. Mazzotti and T. Ritter, *Nat. Chem.*, 2016, **8**, 810–815.
- 17 N. A. Romero, K. A. Margrey, N. E. Tay and D. A. Nicewicz, *Science*, 2015, **349**, 1326–1330.
- 18 W. S. Ham, J. Hillenbrand, J. Jacq, C. Genicot and T. Ritter, *Angew. Chem., Int. Ed.*, 2019, **58**, 532–536.
- 19 S. L. Rössler, B. J. Jelier, P. F. Tripet, A. Shemet, G. Jeschke, A. Togni and E. M. Carreira, *Angew. Chem., Int. Ed.*, 2019, **58**, 526–531.
- 20 A. Ruffoni, F. Juliá, T. D. Svejstrup, A. J. McMillan, J. J. Douglas and D. Leonori, *Nat. Chem.*, 2019, **11**, 426–433.

21 A. Ajaz, E. C. McLaughlin, S. L. Skraba, R. Thamatam and R. P. Johnson, *J. Org. Chem.*, 2012, **77**, 9487–9495.

22 C. Odena, E. Gómez-Bengoa and R. Martin, *J. Am. Chem. Soc.*, 2023, **146**, 112–117.

23 Y. Sekiguchi, P. Onnuch, Y. Li and R. Y. Liu, *J. Am. Chem. Soc.*, 2024, **147**, 1224–1230.

24 K. Inoue and K. Okano, *ChemCatChem*, 2024, **16**, e202400408.

25 T. Sammakia, E. L. Stangeland and M. C. Whitcomb, *Org. Lett.*, 2002, **4**, 2385–2388.

26 M. Schnürch, M. Spina, A. F. Khan, M. D. Mihovilovic and P. Stanetty, *Chem. Soc. Rev.*, 2007, **36**, 1046–1057.

27 T. R. Puleo and J. S. Bandar, *Chem. Sci.*, 2020, **11**, 10517–10522.

28 K. Inoue, A. Mori and K. Okano, *Org. Lett.*, 2023, **25**, 6693–6698.

29 K. Inoue, A. Mori and K. Okano, *Chem.-Eur. J.*, 2024, **30**, e202400104.

30 M. Kubo, N. Inayama, E. Ota and J. Yamaguchi, *Org. Lett.*, 2022, **24**, 3855–3860.

31 K. Matsushita, R. Takise, K. Muto and J. Yamaguchi, *Sci. Adv.*, 2020, **6**, eaba7614.

32 S. Edelmann and J.-P. Lumb, *Nat. Chem.*, 2024, **16**, 1193–1199.

33 B. Li, A. Ruffoni and D. Leonori, *Angew. Chem., Int. Ed.*, 2023, **62**, e202310540.

34 R. Mykura, R. Sánchez-Bento, E. Matador, V. K. Duong, A. Varela, L. Angelini, R. J. Carbo, J. Llaveria, A. Ruffoni and D. Leonori, *Nat. Chem.*, 2024, **16**, 771–779.

35 S. C. Patel and N. Z. Burns, *J. Am. Chem. Soc.*, 2022, **144**, 17797–17802.

36 T. J. Pearson, R. Shimazumi, J. L. Driscoll, B. D. Dherange, D.-I. Park and M. D. Levin, *Science*, 2023, **381**, 1474–1479.

37 R. Sánchez-Bento, B. Roure, J. Llaveria, A. Ruffoni and D. Leonori, *Chem.*, 2023, **9**, 3685–3695.

38 B. Iddon, O. Meth-Cohn, E. Scriven, H. Suschitzky and P. Gallagher, *Angew. Chem., Int. Ed.*, 1979, **18**, 900–917.

39 R. A. Odum and A. M. Aaronson, *J. Am. Chem. Soc.*, 1969, **91**, 5680–5681.

40 L. Horner and A. Christmann, *Angew. Chem., Int. Ed.*, 1963, **2**, 599–608.

41 N. Gritsan and M. Platz, *Chem. Rev.*, 2006, **106**, 3844–3867.

42 N. P. Gritsan, T. Yuzawa and M. S. Platz, *J. Am. Chem. Soc.*, 1997, **119**, 5059–5060.

43 N. P. Gritsan, Z. Zhu, C. M. Hadad and M. S. Platz, *J. Am. Chem. Soc.*, 1999, **121**, 1202–1207.

44 A. Marcinek, M. S. Platz, S. Y. Chan, R. Floresca, K. Rajagopalan, M. Golinski and D. Watt, *J. Phys. Chem.*, 1994, **98**, 412–419.

45 H. Takeuchi and K. Koyama, *J. Chem. Soc., Chem. Commun.*, 1981, 202–204.

46 T. B. Brown, P. R. Lowe, C. H. Schwalbe and M. F. Stevens, *J. Chem. Soc., Perkin Trans.*, 1983, **1**, 2485–2490.

47 O. L. Chapman and J. P. Le Roux, *J. Am. Chem. Soc.*, 1978, **100**, 282–285.

48 W. T. Borden, N. P. Gritsan, C. M. Hadad, W. L. Karney, C. R. Kemnitz and M. S. Platz, *Acc. Chem. Res.*, 2000, **33**, 765–771.

49 W. L. Karney and W. T. Borden, *J. Am. Chem. Soc.*, 1997, **119**, 1378–1387.

50 N. P. Gritsan, I. Likhotvorik, M.-L. Tsao, N. Çelebi, M. S. Platz, W. L. Karney, C. R. Kemnitz and W. T. Borden, *J. Am. Chem. Soc.*, 2001, **123**, 1425–1433.

51 S. M. Ulfa, H. Okamoto and K. Satake, *Chem. Lett.*, 2012, **41**, 400–402.

52 K. Satake, R. Okuda, M. Hashimoto, Y. Fujiwara, I. Watadani, H. Okamoto, M. Kimura and S. Morosawa, *J. Chem. Soc., Chem. Commun.*, 1991, 1154–1156.

53 B. A. DeGraff, D. W. Gillespie and R. J. Sundberg, *J. Am. Chem. Soc.*, 1974, **96**, 7491–7496.

54 G. Li, M. N. Lavagnino, S. Z. Ali, S. Hu and A. T. Radosevich, *J. Am. Chem. Soc.*, 2022, **145**, 41–46.

55 F. R. Atherton and R. W. Lambert, *J. Chem. Soc., Perkin Trans.*, 1973, **1**, 1079–1084.

56 J. L. Dektar and N. P. Hacker, *J. Am. Chem. Soc.*, 1990, **112**, 6004–6015.

57 E. Despagnet-Ayoub, W. W. Kramer, W. Sattler, A. Sattler, P. J. LaBeaume, J. W. Thackeray, J. F. Cameron, T. Cardolaccia, A. A. Rachford and J. R. Winkler, *Photochem. Photobiol. Sci.*, 2018, **17**, 27–34.

58 Z.-H. Lin, Y.-F. Yao and C.-P. Zhang, *Org. Lett.*, 2022, **24**, 8417–8422.

59 B. Zhang, T. Li and Y. Kang, *Res. Chem. Intermed.*, 2017, **43**, 6617–6625.

60 T. Gendron, K. Sander, K. Cybulski, L. Benhamou, P. K. B. Sin, A. Khan, M. Wood, M. J. Porter and E. Årstad, *J. Am. Chem. Soc.*, 2018, **140**, 11125–11132.

61 F. Sirindil, S. Maher, M. Schöll, K. Sander and E. Årstad, *Int. J. Mol. Sci.*, 2022, **23**, 15481.

62 K. Lamara and R. K. Smalley, *Tetrahedron*, 1991, **47**, 2277–2290.

63 H. Inui, K. Sawada, S. Oishi, K. Ushida and R. J. McMahon, *J. Am. Chem. Soc.*, 2013, **135**, 10246–10249.

64 C. M. Nunes, I. Reva, S. Kozuch, R. J. McMahon and R. Fausto, *J. Am. Chem. Soc.*, 2017, **139**, 17649–17659.

65 T. Schleif, J. Mieres-Perez, S. Henkel, E. Mendez-Vega, H. Inui, R. J. McMahon and W. Sander, *J. Org. Chem.*, 2019, **84**, 16013–16018.

66 Y. Ohba, S. Kubo, M. Nakai, A. Nagai and M. Yoshimoto, *Bull. Chem. Soc. Jpn.*, 2006, **59**, 2317–2320.

67 J. P. Horwitz, V. K. Iyer, H. B. Vardhan, J. Corombos and S. C. Brooks, *J. Med. Chem.*, 1986, **29**, 692–698.

68 M. H. Aukland, M. Šiaučiulis, A. West, G. J. Perry and D. J. Procter, *Nat. Catal.*, 2020, **3**, 163–169.

69 F. Berger, M. B. Plutschack, J. Riegger, W. Yu, S. Speicher, M. Ho, N. Frank and T. Ritter, *Nature*, 2019, **567**, 223–228.

70 A. Dewanji, L. van Dalsen, J. A. Rossi-Ashton, E. Gasson, G. E. Crisenza and D. J. Procter, *Nat. Chem.*, 2023, **15**, 43–52.

71 P. S. Engl, A. P. Häring, F. Berger, G. Berger, A. Pérez-Bitrián and T. Ritter, *J. Am. Chem. Soc.*, 2019, **141**, 13346–13351.

72 J. Li, J. Chen, R. Sang, W.-S. Ham, M. B. Plutschack, F. Berger, S. Chabba, A. Schnegg, C. Genicot and T. Ritter, *Nat. Chem.*, 2020, **12**, 56–62.

73 L. van Dalsen, R. E. Brown, J. A. Rossi-Ashton and D. J. Procter, *Angew. Chem., Int. Ed.*, 2023, **62**, e202303104.

74 D. Zhao, R. Petzold, J. Yan, D. Muri and T. Ritter, *Nature*, 2021, **600**, 444–449.

